

An Effective Quantum Potential for Particle-Particle Interactions in Three-dimensional Semiconductor Device Simulations

Clemens Heitzinger and Christian Ringhofer

Department of Mathematics and Statistics
Arizona State University, Tempe, AZ 85287, USA

Email: Clemens.Heitzinger@ASU.edu

Abstract

The classical Coulomb potential and force can be calculated efficiently using fast multi-pole methods. Effective quantum potentials, however, describe the physics of electron transport in semiconductors more precisely. Such an effective quantum potential was derived previously for the interaction of an electron with a barrier for use in particle-based Monte Carlo semiconductor device simulators. The method is based on a perturbation theory around thermodynamic equilibrium and leads to an effective potential scheme in which the size of the electron depends upon its energy and which is parameter-free. Here we extend the method to electron-electron interactions and show how the effective quantum potential can be evaluated efficiently in the context of many-body problems. Finally several examples illustrate how the momentum of the electrons changes the classical potential.

Contents

| | | |
|----------|---|-----------|
| 1 | Introduction | 3 |
| 2 | The Effective Quantum Potential for the N-body Problem | 4 |
| 3 | Evaluation of the N-body Effective Quantum Potential | 7 |
| 3.1 | General Remarks Concerning the Many-body Problem . . . | 7 |
| 3.2 | Evaluation of the Effective Quantum Potential in 3D | 8 |
| 4 | Properties of the 3D N-body Effective Quantum Potential | 12 |
| 5 | Conclusion | 14 |
| 6 | Acknowledgment | 15 |

1 Introduction

As the gate lengths of semiconductor devices are scaled into the deca-nanometer regime, the quantum-mechanical nature of carrier transport becomes more and more important. State-of-the-art physical device simulators, like Ensemble Monte Carlo simulators, must take quantum-mechanical effects into account, as opposed to the classical treatment of electron interactions by the Coulomb potential.

An approach that lends itself to the inclusion in Monte Carlo simulators are so-called effective quantum potentials. The main idea is to replace the action of the Hamiltonian on the wave functions in the Wigner formulation by the action of the classical Hamiltonian on particles with a modified potential. In other words the classical Coulomb potential is replaced by a quantum-corrected one.

The pseudo-differential operator (PDO) for the effective quantum potential we build on here is based on a perturbation theory around thermal equilibrium [1,2], was first derived in [3], and used to include the interaction between potential wells and single electrons in previous work [4,5]. This paper is concerned with the generalization of the approach in [3] to the general N -body problem.

Other approaches to the inclusion of quantum-mechanical size-quantization effects that have been proposed are an effective potential due to Ferry [6] and the density gradient method [7,8]. In both there are a number of parameters that do not represent exact physical values, like the size of the electron wave-packet in the effective potential approach and the mass of the carriers in the density gradient methods. An alternative is the direct particle simulation of the dynamics of wave-packets on highly unstructured meshes [9,10]. The effective quantum potential we use here does not depend on parameters that are hard to estimate and is also generally smoother than the classical potential by two degrees, i.e., two more classical derivatives exist which relieves the problem of statistical noise.

The paper is organized as follows. After the derivation of the effective quantum potential for the N -body problem in three spatial dimensions in Section 2, we describe in Section 3 how the associated pseudo-differential operator can be evaluated efficiently. Finally we discuss some properties of the potential in Section 4. Examples of using the effective quantum potential in an Ensemble Monte Carlo device simulator were published in [11].

2 The Effective Quantum Potential for the N -body Problem

The idea of the effective potential approach is to incorporate quantum mechanical corrections into particle based simulators by modifying the classical forces acting on electrons during free flight. Hence the field term $-e\nabla_x V(x)$ in the semi-classical Boltzmann equation

$$\partial_t f + \nabla_x \left(\frac{1}{m_*} p f \right) - \nabla_p (e f \nabla_x V) = Q(f)$$

is replaced by a modified field term $-e\nabla_x V_Q(x, p, \beta)$. Then the trajectories of the electrons are computed by

$$\frac{dx}{dt} = \frac{p}{m_*}, \quad \frac{dp}{dt} = -e\nabla_x V_Q(x, p, \beta),$$

where the time-dependence of the potential is frozen during the free flight phase. $\beta = 1/(KT)$ is the equilibrium temperature. Given a mean field potential $V(x)$ and a particle at x with momentum p , the quantum potential $V_Q(x, p, \beta)$ is given by the PDO

$$\frac{\sinh\left(\frac{\beta\hbar p \cdot \nabla_x}{2im}\right)}{\frac{\beta\hbar p \cdot \nabla_x}{2im}} \exp\left(\frac{\beta\hbar^2}{8m_*} \Delta_x\right)$$

acting on V , i.e.,

$$V_Q(x, p, \beta) = \frac{\sinh\left(\frac{\beta\hbar p \cdot \nabla_x}{2im}\right)}{\frac{\beta\hbar p \cdot \nabla_x}{2im}} \exp\left(\frac{\beta\hbar^2}{8m_*} \Delta_x\right) V(x). \quad (1)$$

This effective quantum potential was derived first in [3].

For the description of particle-particle interactions beyond standard mean field theory we have to extend this approach to an N -body system. After defining the N -dimensional position and momentum vectors $X := (x_1, \dots, x_N)$ and $P := (p_1, \dots, p_N)$, we start from the N -body Wigner and Bloch equations and obtain the N -particle transport equation

$$\partial_t F + \nabla_P E \cdot \nabla_X F - \nabla_X E \cdot \nabla_P F = 0,$$

where F is the N -dimensional Wigner function and E the effective energy. The Coulomb potential is given by

$$G(X) = \frac{1}{N-1} \sum_{j=2}^N \sum_{k=1}^{j-1} g(x_j - x_k), \quad \Delta_x g = \delta(x). \quad (2)$$

Following the same procedure as in the derivation of (1), we arrive at the N -particle effective energy

$$E = \frac{\|P\|^2}{2m_*} + V_Q(X, P, \beta)$$

and the quantum potential

$$V_Q(X, P, \beta) = \frac{\sinh\left(\frac{\beta\hbar P \cdot \nabla_X}{2im}\right)}{\frac{\beta\hbar P \cdot \nabla_X}{2im}} \exp\left(\frac{\beta\hbar^2}{8m_*} \Delta_X\right) G(x).$$

For notational simplicity we define

$$\Gamma(r, s) := \frac{\sinh\left(\frac{\beta\hbar r}{2m}\right)}{\frac{\beta\hbar r}{2m}} \exp\left(\frac{-\beta\hbar^2}{8m_*} s\right)$$

and hence we have

$$V_Q(X, P, \beta) = \Gamma\left(\frac{1}{i}P \cdot \nabla_X, -\Delta_X\right)G(X).$$

Now the goal is to compute the force acting on one particle, say the one at x_1 . Hence we need $\nabla_{x_1} V_Q(X, P, \beta)$, which is given in the following proposition.

Proposition 2.1 *The quantum force $\nabla_{x_1} V_Q(X, P, \beta)$ acting on the particle at x_1 is given by*

$$\nabla_{x_1} V_Q(X, P, \beta) = \frac{1}{N-1} \sum_{j=2}^N \frac{\sinh\left(\frac{\beta\hbar(p_1-p_j) \cdot \nabla_{x_1}}{2im}\right)}{\frac{\beta\hbar(p_1-p_j) \cdot \nabla_{x_1}}{2im}} \exp\left(\frac{\beta\hbar^2}{4m_*} \Delta_{x_1}\right) \nabla_{x_1} g(x_1 - x_j),$$

where g is the Green function. This can also be written as

$$V_Q(X, P, \beta) = \frac{1}{N-1} \sum_{j=2}^N W(x_1 - x_j, p_1 - p_j)$$

$$W(x, p) := \frac{\sinh\left(\frac{\beta\hbar p \cdot \nabla_x}{2im}\right)}{\frac{\beta\hbar p \cdot \nabla_x}{2im}} \exp\left(\frac{\beta\hbar^2}{4m_*} \Delta_x\right) g(x).$$

The potential is given by

$$V_Q(X, P, \beta) = \frac{1}{N-1} \sum_{j=2}^N \frac{\sinh\left(\frac{\beta\hbar(p_1-p_j) \cdot \nabla_{x_1}}{2im}\right)}{\frac{\beta\hbar(p_1-p_j) \cdot \nabla_{x_1}}{2im}} \exp\left(\frac{\beta\hbar^2}{4m_*} \Delta_{x_1}\right) g(x_1 - x_j).$$

Proof. First we calculate the Fourier transform of the N -body Coulomb potential (2) with respect to X in the dual variable Y . To that end we calculate the transform of $g(x_j - x_k)$ with respect to x_j and x_k . With $d \in \{1, 2, 3\}$, $R := \mathbb{R}^d$, and $c := (2\pi)^{-d/2}$ it equals

$$\begin{aligned} F(g(x_j - x_k))(y_j, y_k) &= c^2 \int_R \int_R g(x_j - x_k) e^{-i(x_j - x_k)y_j - ix_k(y_j + y_k)} dx_j dx_k \\ &= c^2 \int_R \int_R g(z) e^{-izy_j - ix_k(y_j + y_k)} dz dx_k \\ &= c^{-1} \hat{g}(y_j) \delta(y_j + y_k). \end{aligned}$$

Hence the Fourier transform of the Coulomb potential is

$$\hat{G}(Y) = \frac{c^{1-N}}{N-1} \sum_{j=2}^N \sum_{k=1}^{j-1} \hat{g}(y_j) \delta(y_j + y_k) \prod_{r \neq j, k} \delta(y_r).$$

Since the quantum potential is a PDO, the Fourier transform of the quantum potential with respect to X is now given by multiplying $\hat{G}(Y)$ with the symbol $\Gamma(P \cdot Y, \|Y\|_2^2)$ of the PDO. This yields

$$\hat{V}_Q(X, P, \beta) = \frac{c^{1-N}}{N-1} \sum_{j=2}^N \sum_{k=1}^{j-1} \Gamma(y_j(p_j - p_k), 2\|y_j\|^2) \hat{g}(y_j) \delta(y_j + y_k) \prod_{r \neq j, k} \delta(y_r).$$

In order to compute the force, we differentiate with respect to x_1 or multiply the above by iy_1 . Because $iy_1 \delta(y_1) = 0$ holds, all terms of the second sum except the one for $k = 1$ vanish and we obtain

$$iy_1 \hat{V}_Q(X, P, \beta) = \frac{c^{1-N}}{N-1} \sum_{j=2}^N \Gamma(y_j(p_j - p_1), 2\|y_j\|^2) iy_1 \hat{g}(y_j) \delta(y_j + y_1) \prod_{r \neq 1, j} \delta(y_r).$$

We replace y_j by $-y_1$ and note that Γ and \hat{g} are even functions of Y .

$$iy_1 \hat{V}_Q(X, P, \beta) = \frac{c^{1-N}}{N-1} \sum_{j=2}^N \Gamma(y_1(p_j - p_1), 2\|y_1\|^2) iy_1 \hat{g}(y_1) \delta(y_j + y_1) \prod_{r \neq 1, j} \delta(y_r).$$

Computing the inverse Fourier transform now gives

$$\begin{aligned} \nabla_{x_1} V_Q(X, P, \beta) &= \frac{c}{N-1} \sum_{j=2}^N \int_R \Gamma(y_1(p_j - p_1), 2\|y_1\|^2) iy_1 \hat{g}(y_1) e^{iy_1 \cdot (x_1 - x_j)} dy_1 \\ &= \frac{1}{N-1} \sum_{j=2}^N \Gamma\left(\frac{1}{i}(p_1 - p_j) \nabla_{x_1}, -2\Delta_{x_1}\right) \nabla_{x_1} g(x_1 - x_j) \end{aligned}$$

This completes the proof. \blacksquare

3 Evaluation of the N -body Effective Quantum Potential

3.1 General Remarks Concerning the Many-body Problem

The time evolution of an ensemble of N particles connected by a central force can be performed efficiently using the Fast Multi-pole Method (FMM) [12, 13]. This technique has been applied to the three-dimensional Coulomb potential. There are in principle two ways to incorporate an effective quantum potential into an FMM algorithm. One option is to devise an FMM algorithm that works in the whole x - and p -spaces. We discuss this option first.

Since the effective quantum potential from Proposition 2.1 depends on both the x - and p -spaces, an FMM algorithm for three-dimensional structures works in a six-dimensional space. Although FMM algorithms work in $O(n)$ time where n is the number of particles, they are faster than direct summation only if the number of particles considered exceeds a certain minimum. For three-dimensional FMM implementations for the classical Coulomb potential this minimum number can be expected to be around one thousand particles. For a six-dimensional algorithm, however, it will be much higher.

Quantum mechanical corrections to the classical Coulomb potential are only required in small structures. But in small structures there are only few free charges. We can estimate the number of electrons that take part in charge transport in semiconductors roughly as follows. We assume a solubility limit for dopants in silicon of $2 \cdot 10^{26} \text{ m}^{-3}$. Therefore an upper bound for the number of charged particles, electrons and dopants, in a volume of $(10 \text{ nm})^3 = 10^{-24} \text{ m}^3$ (which corresponds to the volume of channels of future MOSFETs) is approximately 400.

Furthermore, an FMM algorithm only makes sense when it works on a hierarchical grid at least three levels deep. In practice the number of levels will have to be higher for a six-dimensional algorithm. Already on the fourth level there are $(2^4)^6 = 2^{24}$ grid cells and the same number of series expansions must be stored. If we assume that in each series expansion four terms are used for each of the six variables plus the mixed terms, this means that $4^6 = 2^{12}$ single floats have to be stored. In summary this implies a memory requirement of $2^{24} \cdot 2^{12} \cdot 4 \text{ byte} = 2^{38} \text{ byte} = 256 \text{ Gb}$ on the fourth level and the same calculation for the third level yields 4Gb. Unless a method is found to further condense the series expansions due to the specific form of the effective potential, this requirement is prohibitive on

current hardware.

Because of these two reasons, the comparatively small number of particles and the enormous memory requirement, a six-dimensional FMM implementation cannot work efficiently. An alternative to the method discussed in this paper is the particle-particle/particle-mesh (P³M) approach [14]. The P³M method was used successfully in three-dimensional semiconductor device simulations with non-periodic boundary conditions [15, 16]. For a six-dimensional problem, however, the P³M approach is not adequate since it involves the pointwise inversion of a six-dimensional field operator to avoid double-counting of charges.

The second option is to treat the short and long range part of the potential differently. The short range part is treated by evaluating the effective quantum potential as a function of position and momentum space and the long range part is treated by evaluating the classical Coulomb potential using an FMM algorithm. This means that we can take advantage of the efficient calculation of the classical potential provided by the FMM algorithm. In the long range interaction the quantum mechanical effects can be neglected as is observed in the convergence properties of the effects quantum potential given in Proposition 2.1.

This allows to reduce the number of dimensions and work with an essentially three-dimensional FMM algorithm. In future devices it is even possible to solve the N -body problem by direct summation, since the number of electrons is in the hundreds.

3.2 Evaluation of the Effective Quantum Potential in 3D

Here we show how in three spatial dimensions the evaluation of the six-dimensional integral of the PDO can be reduced to a two-dimensional integral. These integrals can be evaluated without numerical problems and can also be tabulated for use in three-dimensional particle-based Monte Carlo semiconductor device simulators. The external bias and the doping are constant throughout a Monte Carlo simulation and can therefore be treated by solving the Poisson equation once at the beginning of a device simulation run.

We start with a few lemmata.

Lemma 3.1 *For a function of a three-dimensional vector that only depends on its length, i.e., $f(\mathbf{r}) = f(\|\mathbf{r}\|)$, the Fourier transform can be calculated using the*

formula

$$\int_{\mathbb{R}^3} f(\|\mathbf{r}\|) e^{\pm i\mathbf{k}\cdot\mathbf{r}} d\mathbf{r} = \frac{4\pi}{\|\mathbf{k}\|} \int_0^\infty r f(r) \sin(r\|\mathbf{k}\|) dr.$$

Lemma 3.2 The Fourier transform of $1/\|x\|$, $x \in \mathbb{R}^3$, in the distributional sense is

$$F\left(\frac{1}{\|x\|}\right)(\xi) = \frac{4\pi}{(2\pi)^{3/2}} \frac{1}{\|\xi\|^2}.$$

Proof. Using Lemma 3.1 we find

$$F\left(\frac{1}{\|x\|}\right)(\xi) = \frac{1}{(2\pi)^{3/2}} \frac{4\pi}{\|\xi\|} \int_0^\infty \sin(\|\xi\|r) dr.$$

For the integral on the right hand side we find in the distributional sense that

$$\begin{aligned} \int_0^\infty \sin(\|\xi\|r) dr &= \frac{1}{2} \int_{-\infty}^\infty \operatorname{sgn}(r) \sin(\|\xi\|r) dr \\ &= \frac{1}{4i} \int_{-\infty}^\infty \operatorname{sgn}(r) \left(e^{i\|\xi\|r} - e^{-i\|\xi\|r} \right) dr \\ &= \frac{\sqrt{2\pi}}{4i} \left(F(\operatorname{sgn}(-x))(\|\xi\|) - F(\operatorname{sgn}x)(\|\xi\|) \right) \\ &= \frac{1}{\|\xi\|}, \end{aligned}$$

where we have used $F(\operatorname{sgn}x)(y) = 2/(\sqrt{2\pi}iy)$ and $F(\operatorname{sgn}(-x)) = -F(\operatorname{sgn}x)$. ■

Lemma 3.3 If $a \in \mathbb{C}$, $\Re(a) \geq 0$, and $b \in \mathbb{R}$, then

$$\int_0^\infty \frac{1}{r} \exp(-ar^2) \sin(br) dr = \frac{\pi}{2} \operatorname{erf}\left(\frac{b}{2\sqrt{a}}\right),$$

where erf is the error function with $\operatorname{erf}(-\infty) = -1$ and $\operatorname{erf}(\infty) = 1$.

Proof. The identity can be deduced by writing the integral in the form

$$\frac{1}{2} \int_{-\infty}^\infty \frac{1}{r} \exp(-ar^2) \frac{\exp(ibr) - \exp(-ibr)}{2i} dr$$

and using the Fourier transformation. ■

Lemma 3.4 *If $a \in \mathbb{C}$, $\Re(a) \geq 0$, and $c \in \mathbb{R}^+$, then*

$$\int_{\mathbb{R}} \frac{e^{-ar^2}}{r^2 + c} dr = \frac{\pi e^{ac} \operatorname{erfc}(\sqrt{ac})}{\sqrt{c}},$$

where $\operatorname{erfc} := 1 - \operatorname{erf}$ is the complementary error function.

The Green function $g : \mathbb{R}^3 \rightarrow \mathbb{R}$ is a solution of $\Delta_x g(x) = \delta(x)/\varepsilon_0$. In three spatial dimensions we find

$$g(x) := -\frac{1}{4\pi\varepsilon_0 \|x\|}, \quad x \in \mathbb{R}^3. \quad (3)$$

In order to calculate the quantum potential caused by a particle at \bar{x} acting on a particle at x we apply the PDO from Proposition 2.1 to g . Using Lemma 3.2 we calculate the Fourier transform of $g(x - \bar{x})$ as

$$F(g(x - \bar{x}))(\xi) = -\frac{1}{4\pi\varepsilon_0} e^{-i\bar{x} \cdot \xi} F\left(\frac{1}{\|x\|}\right)(\xi) = -\frac{1}{(2\pi)^{3/2}\varepsilon_0} \frac{e^{-i\bar{x} \cdot \xi}}{\|\xi\|^2}.$$

The numerical values of the constants are $m = 9.10938 \cdot 10^{-31}$ kg for the electron mass, $m_* = 6^{2/3}(0.91 \cdot 0.19^2)^{1/3}m \approx 1.05751m$ for the effective electron mass in silicon, $\hbar = 1.05457 \cdot 10^{-34}$ Js, and $\beta = 40$ eV $^{-1}$.

Hence we have

$$\begin{aligned} V_Q((x, \bar{x}), (p, \bar{p}), \beta) &= \frac{\sinh\left(\frac{\beta\hbar(p-\bar{p}) \cdot \nabla_x}{2im}\right)}{\frac{\beta\hbar(p-\bar{p}) \cdot \nabla_x}{2im}} \exp\left(\frac{\beta\hbar^2}{4m_*} \Delta_x\right) g(x - \bar{x}) \\ &= -\frac{1}{(2\pi)^3 \varepsilon_0} \int_{\mathbb{R}^3} \frac{1}{\|\xi\|^2} \frac{\sinh\left(\frac{\beta\hbar}{2m}(p-\bar{p}) \cdot \xi\right)}{\frac{\beta\hbar}{2m}(p-\bar{p}) \cdot \xi} \exp\left(i(x-\bar{x}) \cdot \xi - \frac{\beta\hbar^2}{4m_*} \|\xi\|^2\right) d\xi. \end{aligned}$$

This integrand cannot be integrated elementarily in the sense of the Risch algorithm. $x \neq \bar{x}$ always holds and for now we assume $p \neq \bar{p}$. We introduce a new basis (q_0, z_0, u_0) by setting $y := x - \bar{x}$, $q := p - \bar{p}$, $y_0 := y/\|y\|$, and $q_0 := q/\|q\|$. We can write y as $y = aq_0 + z$, where $q \cdot z = 0$. Setting $z_0 := z/\|z\|$ we have

$$y = aq_0 + bz_0,$$

$a = y \cdot q_0$, $b = y \cdot z_0$, and $a^2 + b^2 = \|y\|^2$. For the angle $\theta := \angle(y, q)$ between $x - \bar{x}$ and $p - \bar{p}$ we find $\alpha := \cos \angle(y, q) = y_0 \cdot q_0 = a/\|y\|$ and without loss of generality $b \geq 0$. The last basis vector u_0 is defined by $u_0 := q_0 \times z_0$. Now we define a unitary transformation A as

$$A : \quad e_1 \mapsto q_0, \quad e_2 \mapsto z_0, \quad e_3 \mapsto u_0.$$

We transform the integration variable ξ by $\eta := A^{-1}\xi$. Hence we find $A^T A = I$, $\xi = A\eta$, $\|\xi\| = \|\eta\|$, $q \cdot \xi = q^T A\eta = (A^T q)^T \eta = \|q\|\eta_1$, and $q \cdot \xi = y^T A\eta = (Q^T y)^T \eta = (aA^T q_0 + bA^T z_0)^T \eta = a\eta_1 + b\eta_2$.

Now the potential reads

$$V_Q((x, \bar{x}), (p, \bar{p}), \beta) = -\frac{1}{(2\pi)^3 \varepsilon_0} \int_{\mathbb{R}^3} \frac{1}{\|\eta\|^2} \frac{\sinh\left(\frac{\beta\hbar}{2m}\|q\|\eta_1\right)}{\frac{\beta\hbar}{2m}\|q\|\eta_1} \exp\left(i(a\eta_1 + b\eta_2) - \frac{\beta\hbar^2}{4m_*}\|\eta\|^2\right) d\eta.$$

Using Lemma 3.4 we integrate over η_3 and arrive at

$$V_Q((x, \bar{x}), (p, \bar{p}), \beta) = -\frac{\pi}{(2\pi)^3 \varepsilon_0} \int_{\mathbb{R}^2} \frac{\sinh\left(\frac{\beta\hbar}{2m}\|q\|\eta_1\right)}{\frac{\beta\hbar}{2m}\|q\|\eta_1} \cos(a\eta_1 + b\eta_2) \frac{\operatorname{erfc}\left(\sqrt{\frac{\beta\hbar^2}{4m_*}(\eta_1^2 + \eta_2^2)}\right)}{\sqrt{\eta_1^2 + \eta_2^2}} d\eta_1 d\eta_2.$$

We introduce polar coordinates (r, φ) via $\eta_1 =: r \cos \varphi$ and $\eta_2 =: r \sin \varphi$. This yields

$$V_Q((x, \bar{x}), (p, \bar{p}), \beta) = -\frac{1}{8\pi^2 \varepsilon_0} \int_0^\infty \int_0^{2\pi} \frac{\sinh\left(\frac{\beta\hbar}{2m}\|q\|r \cos \varphi\right)}{\frac{\beta\hbar}{2m}\|q\|r \cos \varphi} \cos(r(a \cos \varphi + b \sin \varphi)) \operatorname{erfc}\left(\sqrt{\frac{\beta\hbar^2}{4m_*}} r\right) d\varphi dr.$$

For numerical work it is advantageous, if not indispensable, to scale the integration variable r . After the substitution $r =: \rho t$, $\rho \in \mathbb{R}$, and renaming $t \mapsto r$ again, we finally have

$$V_Q((x, \bar{x}), (p, \bar{p}), \beta) = V_Q(\|x - \bar{x}\|, \|p - \bar{p}\|, \theta, \beta) = -\frac{\rho}{8\pi^2 \varepsilon_0} \int_0^\infty \int_0^{2\pi} \frac{\sinh\left(\frac{\beta\hbar}{2m}\|q\|\rho r \cos \varphi\right)}{\frac{\beta\hbar}{2m}\|q\|\rho r \cos \varphi} \cos(\|y\|\rho r \cos(\varphi - \theta)) \operatorname{erfc}\left(\sqrt{\frac{\beta\hbar^2}{4m_*}} \rho r\right) d\varphi dr.$$

In the special case $p = \bar{p}$ the potential simplifies to

$$\begin{aligned} V_Q((x, \bar{x}), \beta) &= -\frac{1}{(2\pi)^3 \varepsilon_0} \int_{\mathbb{R}^3} \frac{1}{\|\xi\|^2} \exp\left(i(x - \bar{x}) \cdot \xi - \frac{\beta\hbar^2}{4m_*}\|\xi\|^2\right) d\xi \\ &= -\frac{1}{(2\pi)^3 \varepsilon_0} \frac{4\pi}{\|x - \bar{x}\|} \int_0^\infty \frac{1}{r} \exp\left(-\frac{\beta\hbar^2}{4m_*} r^2\right) \sin(r\|x - \bar{x}\|) dr \\ &= -\frac{1}{4\pi \varepsilon_0} \frac{1}{\|x - \bar{x}\|} \operatorname{erf}\left(\frac{\|x - \bar{x}\|}{\sqrt{\frac{\beta}{m_*} \hbar}}\right), \end{aligned}$$

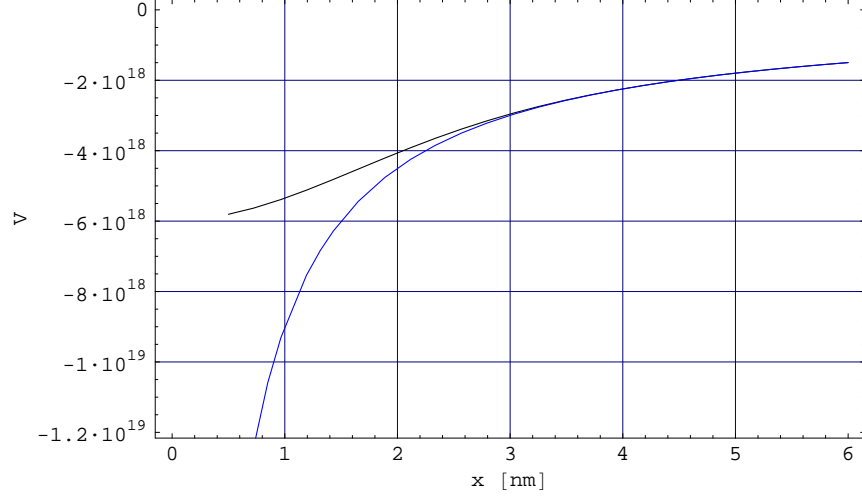


Figure 1: This plot shows the classical Coulomb potential (blue) and the effective quantum potential (black) in the case of particles with identical momentum.

where we have used Lemma 3.1 and Lemma 3.3. For the classical limit we find, as expected,

$$\lim_{\hbar \rightarrow 0} V_Q((x, \bar{x}), \beta) = -\frac{1}{4\pi\epsilon_0} \frac{1}{\|x - \bar{x}\|}.$$

Finally we mention that the derivation of the potential builds on the Green function given in (3). Depending on the device under consideration, the method of image charges can be used to include discontinuities in the permittivity and the presence of metallic contacts. In the case of complicated geometries, it may be non-trivial to apply this method.

4 Properties of the 3D N -body Effective Quantum Potential

We now have a look at the effective quantum potential for particle-particle interactions. In Figure 1 we observe that in the case of particles with identical momentum the classical Coulomb potential and the effective quantum potential are nearly identical for distances greater than about 5 nm. Below that distance the interaction between particles is much less in the quantum mechanical case than in the classical case.

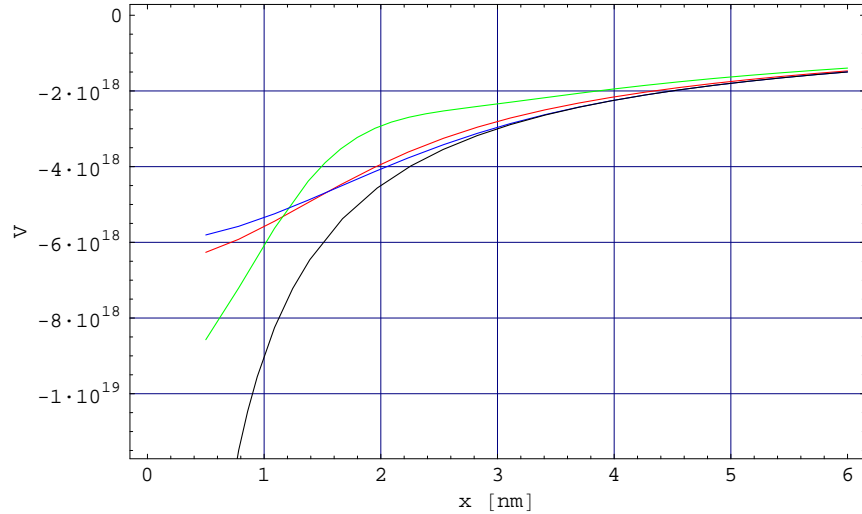


Figure 2: This plot shows the effective quantum potential for a highly energetic electron ($p_x = 10^{-25}$ kg m/s) and a resting one (red); for two highly energetic electrons moving in opposite directions ($p_x = 10^{-25}$ kg m/s and $p_x = -10^{-25}$ kg m/s, green); the effective quantum potential for particles with identical momentum (blue); and the classical Coulomb potential (black).

In the next step we look at the situation of particles with different momentums. In Figure 2 we compare the effective quantum potential for a highly energetic electron and a resting one, for two highly energetic electrons moving in opposite directions, the effective quantum potential for particles with identical momentum, and the classical Coulomb potential. We see that up to relatively long distances (compared to device diameters) the quantum mechanical effects and the especially the influence of the momentum difference have a significant effect. In the figures we also observe – as expected – that the effective quantum potential converges to the classical potential as the distance between particles increases.

In the next figures, Figure 3 and Figure 4, we plot the effective quantum potential as a function of the distance between two particles. In the first case the momentums are $(p, 0, 0)$ and $(-p, 0, 0)$ and in the second case they are $(0, p, 0)$ and $(0, -p, 0)$. As it can be seen, the momentum and angle dependence changes the forces two particles exert on one another in the short range. Depending on distance, angle, and momentum the force can increase or decrease.

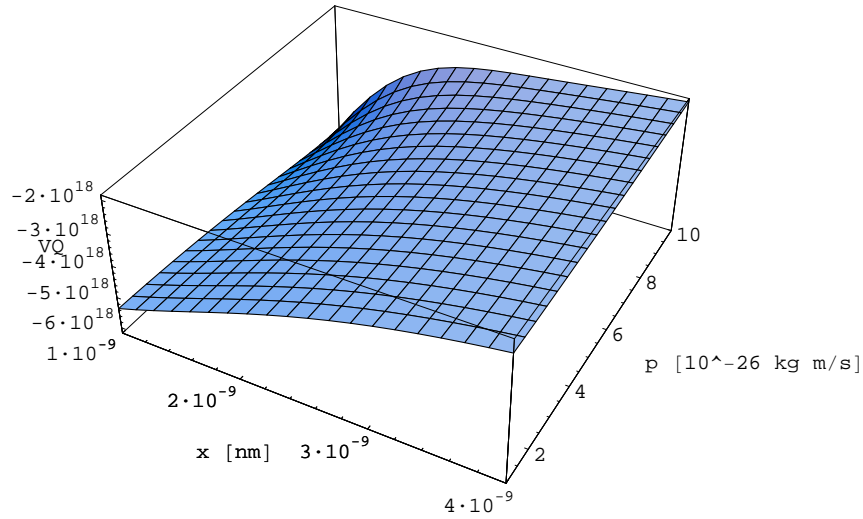


Figure 3: This plot shows the effective quantum potential as a function of distance and momentum for two particles with momentum $p_x = p$ and $p_x = -p$.

5 Conclusion

A parameter-free effective quantum potential for the N -body problem was derived. We focused on the three-dimensional case, since it is the most important one for physically sound semiconductor device simulations. In three spatial dimensions, the six-dimensional PDO can be reduced to a two-dimensional integral. After tabulation this potential can be used in Ensemble Monte Carlo simulations and its evaluation poses no problem on today's computing resources.

Finally we showed how the effective quantum potential depends on the momentum of two interacting electrons and compared it to the classical Coulomb potential which demonstrated considerable differences in the range up to approximately 10 nm.

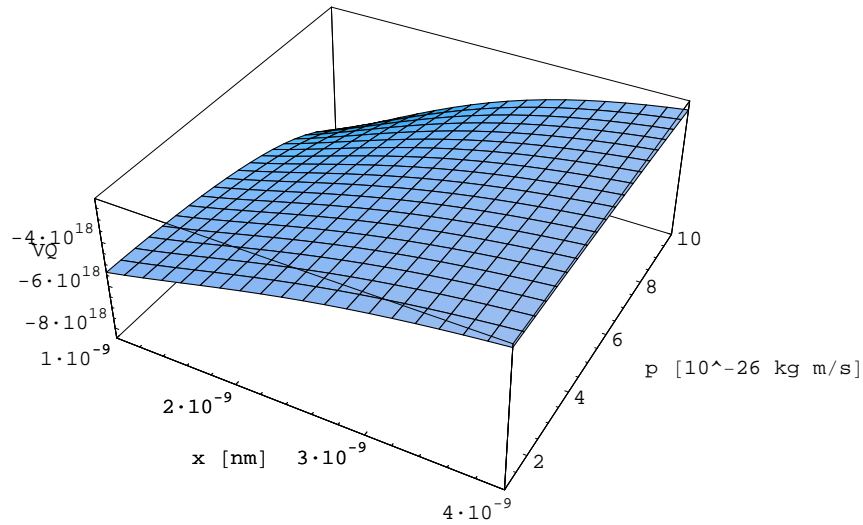


Figure 4: This plot shows the effective quantum potential as a function of distance and momentum for two particles with momentum $p_y = p$ and $p_y = -p$.

6 Acknowledgment

The first author acknowledges support by the Austrian Science Fund (Fonds zur Förderung der wissenschaftlichen Forschung, FWF) via an Erwin Schrödinger Fellowship. The second author acknowledges support through National Science Foundation grant DECS-0218008.

References

- [1] I. Gasser and A. Jünger. The quantum hydrodynamic model for semiconductors in thermal equilibrium. *Z. Angew. Math. Phys.*, 48:45–59, 1997.
- [2] C.L. Gardner and C. Ringhofer. Smooth quantum potential for the hydrodynamic model. *Physical Review*, E53:157–167, 1996.
- [3] C. Ringhofer, C. Gardner, and D. Vasileska. Effective potentials and quantum fluid models: a thermodynamic approach. *Inter. J. on High Speed Electronics and Systems*, 13(3):771–801, 2003.
- [4] Shaikh Ahmed, Dragica Vasileska, Clemens Heitzinger, and Christian Ringhofer. Quantum potential approach to modeling nanoscale MOS-FETs. *Journal of Computational Electronics*, 4(1-2):57–61, 2005.
- [5] Dragica Vasileska, Hasanur Khan, Shaikh Ahmed, Christian Ringhofer, and Clemens Heitzinger. Quantum and Coulomb effects in nanodevices. *International Journal of Nanoscience*, 4(3):305–361, 2005.
- [6] D.K. Ferry. The onset of quantization in ultra-submicron semiconductor devices. *Superlattices & Microstructures*, 27:61, 2000.
- [7] D. Ferry and H. Grubin. Modelling of quantum transport in semiconductor devices. *Solid State Phys.*, 49:283–448, 1995.
- [8] G.J. Iafrate, H.L. Grubin, and D.K. Ferry. Utilization of quantum distribution functions for ultra-submicron device transport. *Journal de Physique*, 42(Colloque C7):307–312, 1981.
- [9] R.E. Wyatt. Quantum wavepacket dynamics with trajectories: Wavefunction synthesis along quantum paths. *Chem. Phys. Lett.*, 313:189–197, 1999.
- [10] R.E. Wyatt. Quantum wave packet dynamics with trajectories: Application to reactive scattering. *J. Chem. Phys.*, 111:4406–4413, 1999.
- [11] Clemens Heitzinger, Christian Ringhofer, Shaikh Ahmed, and Dragica Vasileska. Three-dimensional Monte-Carlo device simulations using an effective quantum potential including electron-electron interactions. *Journal of Computational Electronics*, 2006. (In print).

- [12] L. Greengard and V. Rokhlin. A fast algorithm for particle simulations. *J. Comput. Phys.*, 73(2):325–348, 1987.
- [13] H. Cheng, L. Greengard, and V. Rokhlin. A fast adaptive multipole algorithm in three dimensions. *J. Comput. Phys.*, 155(2):468–498, 1999.
- [14] R.W. Hockney and J.W. Eastwood. *Computer Simulation Using Particles*. McGraw-Hill, New York, 1981.
- [15] W.J. Gross, D. Vasileska, and D.K. Ferry. 3D simulations of ultra-small MOSFETs with real-space treatment of the electron-electron and electron-ion interactions. *VLSI Design*, 10:437, 2000.
- [16] C.J. Wordelman and U. Ravaioli. Integration of a Particle-Particle-Particle-Mesh algorithm with the Ensemble Monte Carlo method for the simulation of ultra-small semiconductor devices. *IEEE Trans. Electron Devices*, 47(2):410–416, 2000.